

# NANOTAILORING STEREOLITHOGRAPHY RESINS FOR UNIQUE APPLICATIONS USING CARBON NANOTUBES

J.H. Sandoval\*, L. Ochoa\*, A. Hernandez\*, O. Lozoya\*  
K.F. Soto†, L.E. Murr†, R.B. Wicker\*

\*University of Texas at El Paso, W.M. Keck Border Biomedical Manufacturing and Engineering Laboratory, Mechanical Engineering, El Paso, Texas 79968

†University of Texas at El Paso, Metallurgical and Materials Engineering, El Paso, Texas 79968

Reviewed, accepted August 3, 2005

## Abstract

Nanostructured materials and exploiting their properties in stereolithography (SL) may open new markets for unique rapidly manufactured functional devices. Controlled amounts of multi-walled carbon nanotubes (MWCNTs) were successfully dispersed in SL epoxy-based resins and complex three-dimensional (3D) parts were successfully fabricated by means of a multi-material SL setup. The effect of the nanosized filler was evaluated using mechanical testing. Small dispersions of MWCNTs resulted in significant effects on the physical properties of the polymerized resin. A MWCNT concentration of .05 wt% (w/v) in DSM Somos® WaterShed™ 11120 resin increased the ultimate tensile stress and fracture stress an average of 17% and 37%, respectively. Electron microscopy was used to examine the morphology of the nanocomposite and results showed affinity between the MWCNTs and SL resin and identified buckled nanotubes that illustrated strong interfacial bonding. These improved physical properties may provide opportunities for using nanocomposite SL resins in end-use applications. Varying types and concentrations of nanomaterials can be used to tailor existing SL resins for particular applications.

*Keywords: rapid prototyping; multi-walled carbon nanotubes; epoxy-based nanocomposite; multiple material stereolithography*

## 1. Introduction

Recent advancements in the synthesis, processing and understanding of nanostructured materials have generated considerable interest in the materials research community. Since the discovery of carbon nanotubes (CNTs), researchers have been investigating methods for exploiting the extraordinary properties of CNTs. CNTs and, more specifically, single-walled CNTs are characterized by an exceptionally high aspect ratio (~1000:1), very low density, a high strength (tensile strength ~ 100 GPa), high stiffness (above 1000 GPa) and the capability to conduct electricity (resistivity ~ 0.5μΩm or less depending on tube diameter) [1]. These characteristics make CNTs ideal candidates for polymer reinforcement. Seeding CNTs in a polymer matrix could potentially increase the mechanical strength of the polymer, introduce electrical conductivity [2, 3] or simply improve the polymer's mechanical behavior and integrity at higher temperatures.

The objective of this research was to investigate tailoring the physical properties of existing epoxy-based resins by dispersing controlled amounts of multi-walled carbon nanotubes (MWCNTs) in the polymeric resin matrix. These epoxy-based resins are used as the build

materials in stereolithography (SL), one of the most popular and accurate rapid prototyping (RP) systems available today. This research was aimed at developing novel nanocomposite resins for specific high performance and functional SL applications.

## Experimental Setup and Procedure

### 2.1 Materials and equipment

A commercially available epoxy-based SL resin, DSM Somos<sup>®</sup> WaterShed<sup>™</sup> 11120, was used as the nanocomposite's matrix material. The MWCNTs used in this research (nanocomposite's filler) were produced by a chemical vapor deposition (CVD) process using a ceramic oxide support. The MWCNTs were then purified by means of acid etching to 95 % (by mass). According to the manufacturer (NanoLab, Inc. Newton, MA), the MWCNTs were characterized by a mean outer diameter of  $30 \pm 15$  nm and a length of 5-20 microns, which represents an actual surface area of  $\sim 220$  m<sup>2</sup> per gram of nanotubes. A sample of MWCNTs was prepared on silicon monoxide/formvar-coated Cu mesh grids and examined under transmission electron microscopy (TEM) using a Hitachi H-8000 analytical TEM. The TEM was fitted with a Noran energy-dispersive (X-ray) spectrometer (EDS) system with a goniometer-tilt stage, operated at 200 kV accelerating potential. A TEM micrograph of the purchased raw material and its diffraction pattern was obtained and shown in Figure 1 to verify that the materials used in this project were indeed MWCNTs.

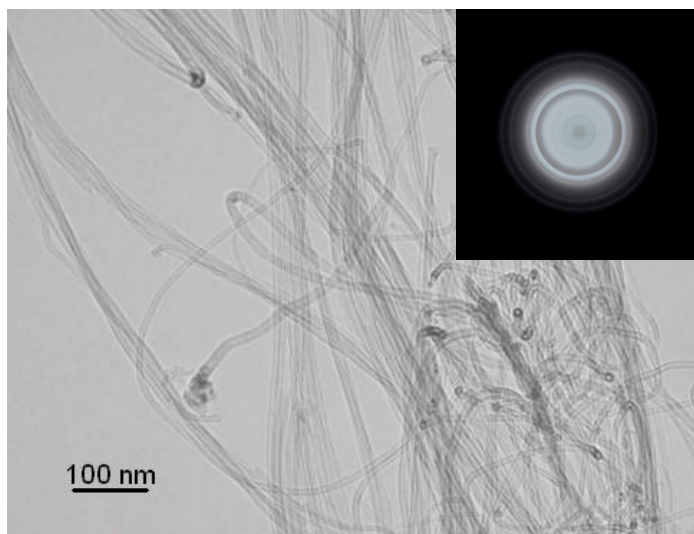


**Figure 1. TEM micrograph and diffraction pattern of MWCNTs.**

A modified 3D Systems SL machine (Model 250/50) equipped with a DPSS solid-state laser upgrade (wavelength 355 nm) was used in this study. The modifications consisted of removing the sweeping mechanism and the original  $\sim 46$  L vat of material and retrofitting a rotating multi-vat carousel system. The rotating vat carousel is composed of three vats (each  $\sim 750$  mL) distributed circumferentially as depicted in Figure 2 and attached to a manual rotary stage via a shaft. The original 10" by 10" platform was replaced with a smaller 4.5" by 4.5" platform, which was attached to the z-stage via an extended assembly. The center of the smaller platform remained in the center of the build envelope so that the laser's starting location remained

unchanged. The height of the z stage elevator sensor was adjusted and fixed (Min  $z = -1.022''$  and Max  $z = 0.340''$  with respect to the default starting building height) by changing the limit micro-switch located on the z-traverse mechanism.

As depicted in Figure 2, the vats contained a partition that served to separate the main vat chamber from a second overflow vat chamber. This partition also served to maintain a constant resin liquid level by continuously pumping resin into the main vat chamber using a peristaltic pump (Masterflex L/S, Model 7550-30). This recirculation system was crucial for a successful part build since this modified system was not equipped with a recoating or sweeping mechanism. Additional details of this setup are contained in sections to follow, and more complete details of this system can be found in [4 and 6].

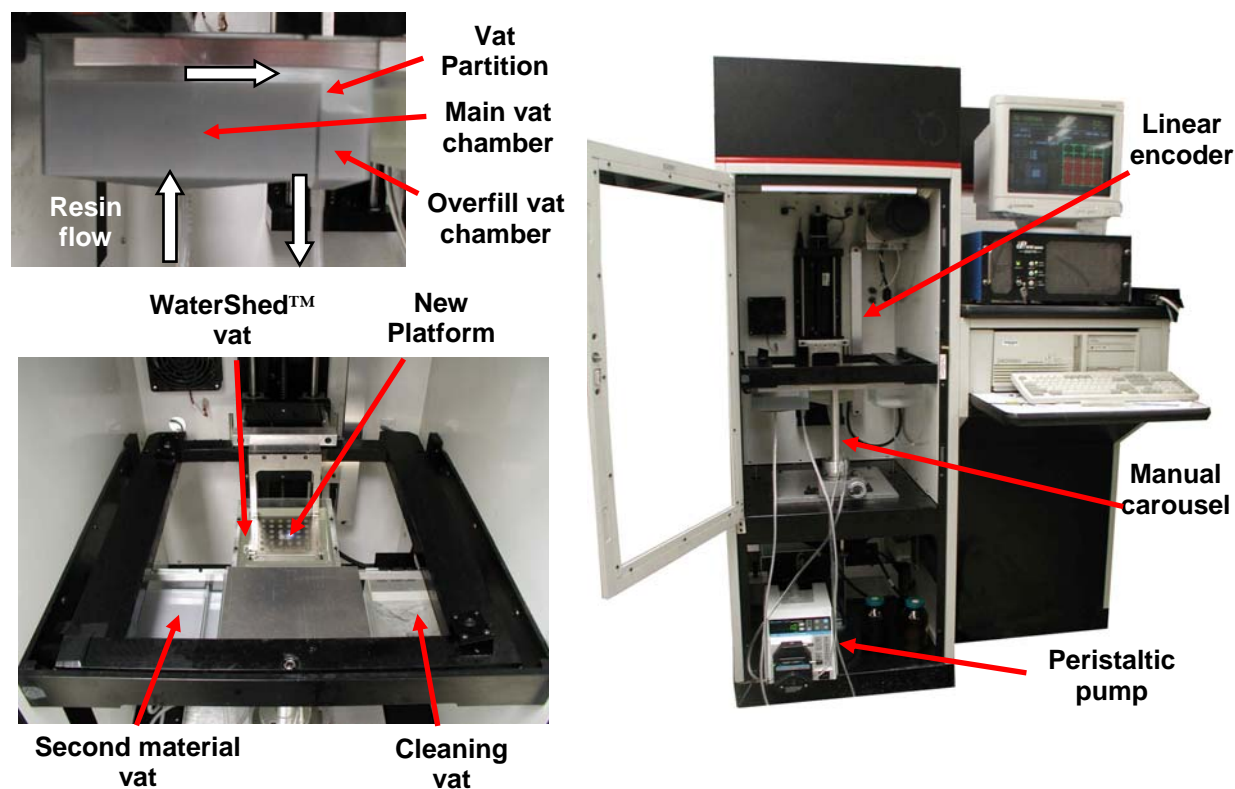


Figure 2. Multiple material SL machine.

The use of this modified SL system allowed for testing of multiple MWCNT concentrations without the need for contaminating and wasting large amounts of both SL resins and nanotubes. More importantly, since this system uses the same controlling software, rim assembly (along with the standard laser sensors) and building SL principles, it allowed effective research and development on the optimal building parameters and concentrations of MWCNTs using relatively small amounts of material (using the ~750 ml vats).

## 2.2 Nanocomposite preparation

The MWCNTs were used as supplied and directly seeded in DSM Somos<sup>®</sup> WaterShed<sup>™</sup> 11120 SL resin by means of shear and ultrasonic dispersion. The mixture was first stirred

mechanically via a paddle until uniformity was achieved. Then, the mixture was ultrasonicated for ~1 hour to diminish the formation of MWCNTs agglomerates. Previous studies suggest negative effects from localized ultrasonic dispersion on CNTs [2, 3, and 10] such as effective length reduction and physical damage to the CNTs' structure. The shear and ultrasonic dispersion techniques used in this research were non-localized. Once dispersed, the solution held a colloidal state for a prolonged period (at least 2 weeks) as no sedimentation was observed in the solution. This is mainly attributed to the viscosity of the SL epoxy resin (~230 cps at 30 °C), which overcomes the attractive forces between CNTs and delays the formation of agglomerates. More importantly, since the ultrasonic dispersion was non-localized, the CNTs' structure was not directly and negatively affected.

The nanocomposite (~750 ml) was then poured into the vat to manufacture sample parts by selectively curing it to a prescribed geometry using standard SL manufacturing in the multiple material SL machine. The peristaltic pump was set to run at 10mL/min to maintain a constant resin level and to provide means for a mechanical, constant mixing and steady recirculation of the nanocomposite. This was one of the main advantages of this modified system as it helped ensure a well-mixed nanocomposite and that no MWCNTs agglomerates were formed. Figure 3 depicts a comparison of pure (semi-transparent) DSM Somos<sup>®</sup> WaterShed<sup>™</sup> 11120 and the same resin containing .05 wt% (w/v) of MWCNTs (opaque).

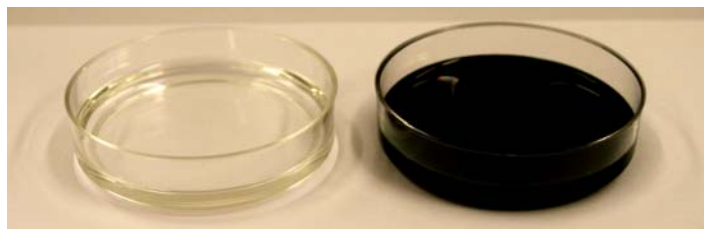


**Figure 3. Petri dishes containing pure DSM Somos<sup>®</sup> WaterShed<sup>™</sup> 11120 (left) and WaterShed<sup>™</sup> 11120 with .05wt% (w/v) of MWCNTs.**

### **3. Results and Discussion**

Once the nanocomposite was prepared, the next step was to select a CAD file and consequently an STL file of a complex 3D geometry to demonstrate the functionality and accuracy of the previously described multi-material SL setup. For this purpose, the chess rook (characterized by many intricate and fine details) that is a common part manufactured by many SL users was selected for demonstration. In addition, several samples were fabricated for mechanical testing and electron microscopy characterization as will be described in the following sections.

#### **3.1 STL and vector files**

One of the restrictions of the multivat SL system is the limited volume available for part building (5" x 5" x 1.5"). Therefore, the original CAD file of the chess rook was scaled down ~70 % to allow for manufacturing within the multi-material SL system. The STL file was then processed within 3D Lightyear where building parameters such as the number of sweeps, pre-dip delay, z-wait, support structure and layer thickness were either modified or eliminated to improve the part's integrity and quality. The 3D Lightyear default value when building (in a

regular SL 250/50) with DSM Somos<sup>®</sup> WaterShed<sup>™</sup> 11120 for z-wait is 10 seconds. At the time the chess rook was manufactured, the multi-material SL system did not use a recoating or sweeping mechanism (which might cause problems such as mounting during the manufacturing process) and thus, the number of sweeps was set to zero. Due to the absence of recoating, the z-wait parameter was also increased to 180 seconds per layer. The support and base structures were also eliminated in this step (within 3D Lightyear) to avoid complications upon part removal from the platform, improve the surface finish of the part, and ease the cleaning process [4, 5]. Finally, the layer thickness was set to  $\sim 0.008''$ , although as described in the following section, the layer thickness was manually varied from  $\sim 0.004''$  to  $0.016''$  to avoid part mounting problems.

### 3.2 SL system adjustments

The laser power was set to  $\sim 55$  mW (power measured by the sensors located in the SL system's rim and verified with a power meter) by means of the beam expander, a laser attenuator and tuning of the laser's crystal. Furthermore, the default critical exposure ( $E_c$ ) and penetration depth ( $D_p$ ) parameters for DSM Somos<sup>®</sup> WaterShed<sup>™</sup> 11120, were increased from  $11.5$  mJ/cm<sup>2</sup> and  $.16$  mm, respectively, to  $60$  mJ/cm<sup>2</sup> and  $6.5$  mm, respectively. These increased  $E_c$  and  $D_p$  values were found experimentally using an unmodified 3D systems SL 250/50 and selectively curing  $\sim 10$  mL of the nanocomposite contained in a Petri dish (as shown in Figure 5). The Petri dish technique served to find appropriate  $E_c$  and  $D_p$  values necessary to cure  $\sim 0.008''$  of the nanocomposite. More complete details of this Petri dish technique can be found in [8].

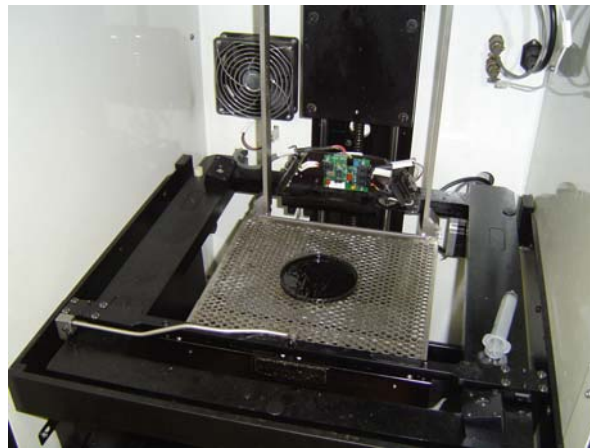
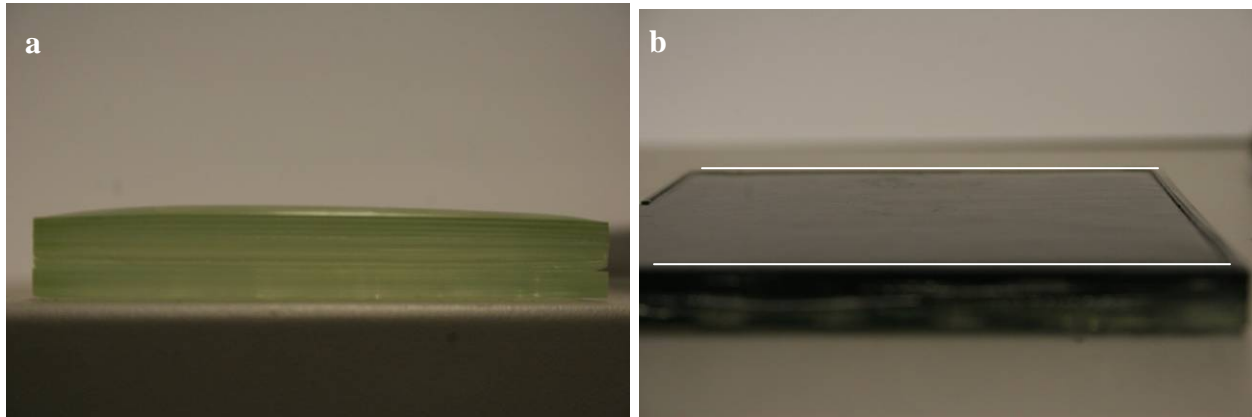


Figure 5. Petri dish containing a sample of the nanocomposite.

Previous studies [4-6] described the need of an intermediate resin platform in order to build with a Mylar sheet and improve the surface finish of the bottom surface of the parts. As mentioned previously, the z-wait parameter was increased to diminish the presence of the resin meniscus over the horizontal surface of the intermediate resin platform. Eliminating part and intermediate platform mounting due to meniscus effects are important for successfully fabricating parts without using the recoating system. Figure 6a demonstrates the formation of an uneven horizontal surface due to the presence of a resin meniscus that resulted in mounting problems and part distortions (due to low or minimum z wait). Figure 6b shows that by simply

increasing the z-wait, a flat surface on the intermediate resin platform (the surface on which a sheet of Mylar is placed for building parts) can be achieved.



**Figure 6. Intermediate resin platforms: (a) built (z wait set to zero) with WaterShed™ 11120 characterized by mounting problems, and (b) built with WaterShed™ 11120 containing .05wt% (w/v) of MWCNT and a z wait of 180 seconds.**

Once the intermediate resin platform was built, a Mylar sheet was placed over it [4, 5]. To ensure proper attachment of the Mylar sheet to the intermediate resin platform and avoid its debonding during the building process of the rook, a border was manufactured around the edge of the intermediate platform. This support structure is highlighted in Figure 6b; its height is equivalent to one layer thickness and was overcured to ensure that existing resin under the Mylar served to bond both surfaces. Once the Mylar was properly secured, the liquid level was adjusted manually and the building process was started. During the building process, the parts were visually inspected to ensure that no part delamination or other part distortions were occurring. The approximate build time for a 1" high rook was ~3 hours. Once the part was completed, the Mylar sheet was removed from the intermediate resin platform, and the part was removed from the Mylar sheet, cleaned with isopropyl alcohol and postcured for 30 minutes in a UV oven. The final product can be observed in Figure 7.

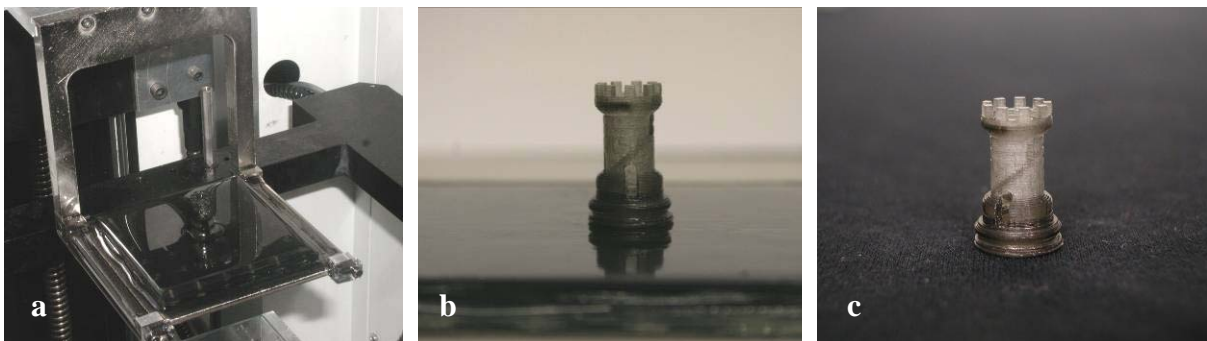


**Figure 7. Building the chess rook on an intermediate resin platform: (a) the resin platform, (b) the part attached to the intermediate resin platform via a Mylar sheet, and (c) the final product.**

### 3.3 Mechanical testing

To measure the effect of dispersing MWCNTs in DSM Somos<sup>®</sup> WaterShed<sup>™</sup> 11120 SL resin on the mechanical properties of the resin, five nanocomposite specimens (WaterShed<sup>™</sup> 11120 with .05% (w/v) MWCNTs) and five control samples (WaterShed<sup>™</sup> 11120 without MWCNTs) were manufactured as per ASTM D-638 [9] (type V specimen) in the multi-material setup described previously (see Figure 8). The nanocomposite specimens were mechanically tested for ultimate tensile stress, fracture stress (or breaking strength), and fracture strain (or elongation at break) and hardness. The tensile specimens were cleaned with isopropyl alcohol and post-cured in a UV oven for ~1 hour (~30 minutes each side) and finally tested. The testing was performed with an INSTRON 5500 machine and the cross-head speed during testing was set at .5 in/min.

To further investigate the effect of this particular nanostructure material on the resin, micro-hardness measurements were taken from the samples prior to mechanical testing. Table 1 shows a summary of the test results for pure DSM Somos<sup>®</sup> WaterShed<sup>™</sup> 11120 and the nanocomposite containing .05wt% (w/v) of MWCNTs.

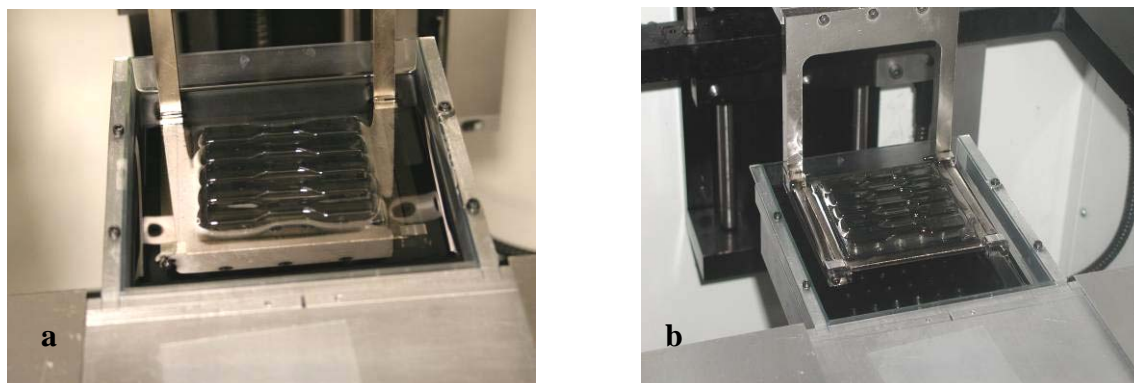


**Figure 8. Building of tensile test samples: (a) WaterShed<sup>™</sup> 11120, and (b) WaterShed<sup>™</sup> 11120 with .05% (w/v) MWCNTs.**

**Table 1. Mechanical testing results.**

Material	Ultimate Tensile Stress (psi)	Standard Deviation (psi)	Fracture Stress (psi)	Standard Deviation (psi)	Fracture Strain (in/in)
WaterShed 11120	6130	168	4200	145	0.14
WaterShed 11120/ MWCNTs (.05wt%)	7355	50	6650	525	0.10

The micro-hardness testing showed an increase (~16%) in the hardness number (Vickers scale) of the nanocomposite when compared to pure WaterShed<sup>™</sup> 11120 (refer to Figure 9). The increase in hardness with the addition of MWCNTs might be explained on the basis of the high stiffness of the nanotubes (typically above 1000 GPa [1]) which reinforced the specimen's

structure and therefore their surface through their 3D random orientation and distribution. Additionally, this nanotube random orientation permits obtaining isotropic properties in the specimens regardless of the orientation on which they are built [11, 12].

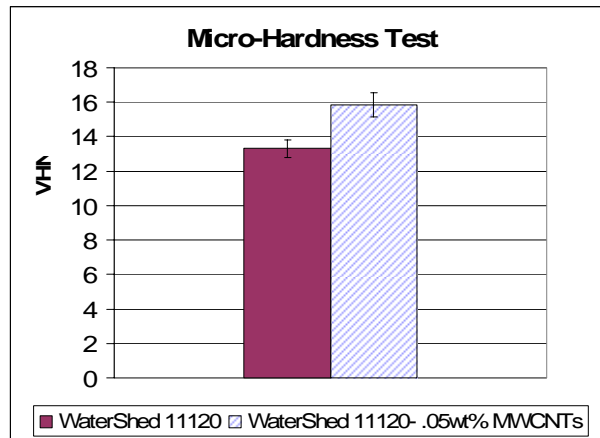


Figure 9 Micro-hardness test results

Concurring with the hardness increase, an average increase of ~17% on the ultimate tensile stress and an increase of ~37% on the fracture or breaking stress was observed in the tested specimens (refer to Figure 10a and b). These improvements suggest an effective load transfer via shearing mechanisms between the polymeric matrix to the randomly distributed filler. However, the nanocomposite specimens experienced a fracture strain decrease of ~30%. As depicted in Figure 10, there has been a drastic reduction in the plastic region shown in the nanocomposite's stress vs. strain curves. This reduction resulted in a brittle type fracture mode for the nanocomposite specimens [11]. Conversely, the pure WaterShed™ 11120 samples observed a ductile fracture mode where macroscopic plastic deformation was observed on the specimens.

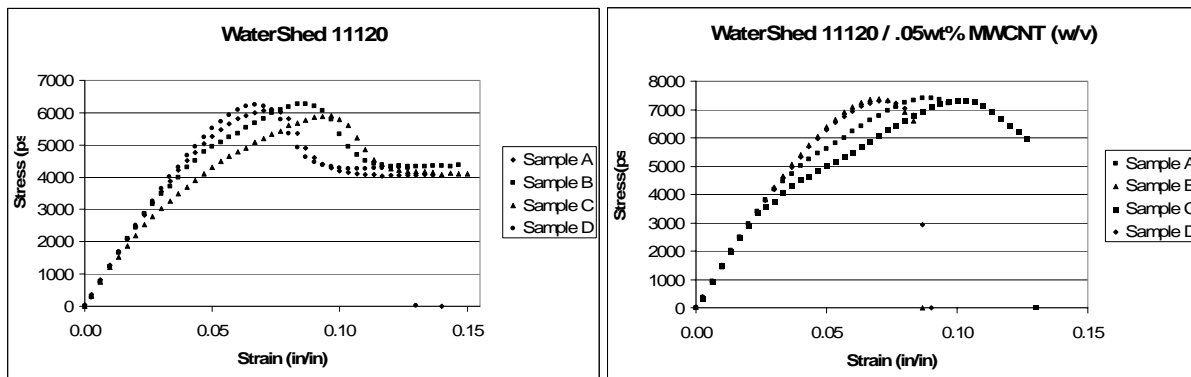
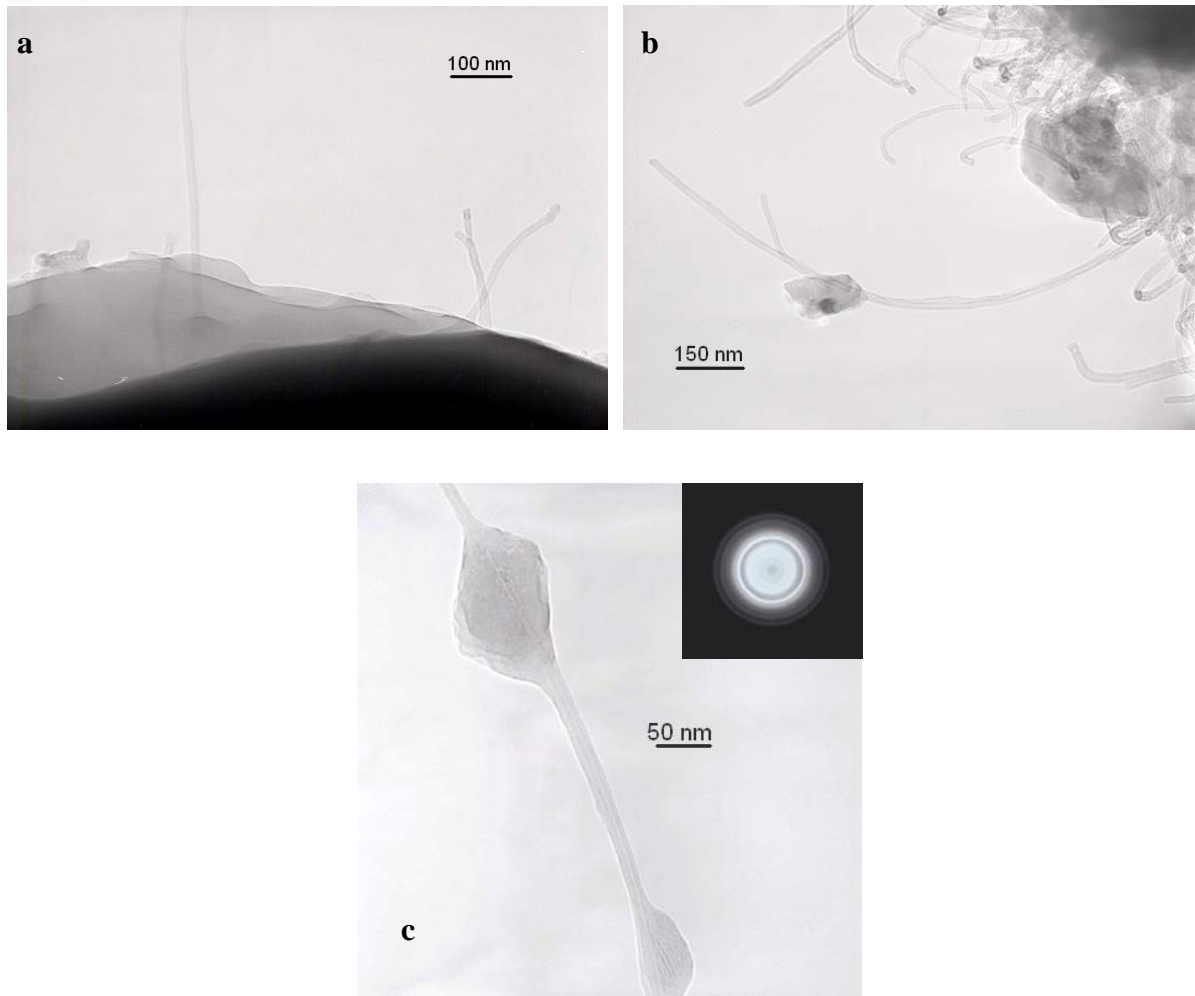


Figure 10. Stress vs. strain results: WaterShed™ 11120 (left), and WaterShed™ 11120 with .05% (w/v) MWCNTs (right). Note the decrease in plastic region of the nanocomposite specimens when compared to pure WaterShed™ 11120.

### 3.4 TEM Characterization

To investigate the interface between the MWCNTs and the SL resin in this novel nanocomposite, samples from the fracture surface of the tensile test specimens were characterized under TEM. The nanocomposite samples were sliced and sandwiched between two 75 square mesh, copper grids and observed in the TEM. These TEM micrographs (Fig.11 a, b and c), show the affinity between the polymeric matrix and the filler. It can be noted that there is good wetting and a strong interfacial bonding between the materials.



**Figure 10. TEM micrographs taken from the fracture surface of the MWCNTs/SL resin nanocomposite test specimen (a, b & c)**

MWCNTs/ matrix pullout effects were not observed during the TEM characterization process. Pullout effects are mainly observed and attributed to a weak MWCNT interface bonding with the polymer matrix. This poor interfacial bonding results in an actual decrease of the mechanical properties of the pure material [11-13]. A very interesting phenomenon was observed in several micrographs of samples that were previously pulled in tensile tests. These micrographs portrayed buckled or collapsed MWCNTs (refer to Fig. 12). It is believed that this

phenomenon was a direct result of the photopolymerization (in the SL machine and in the UV oven), and thermal effects introduced by the SL system's laser.

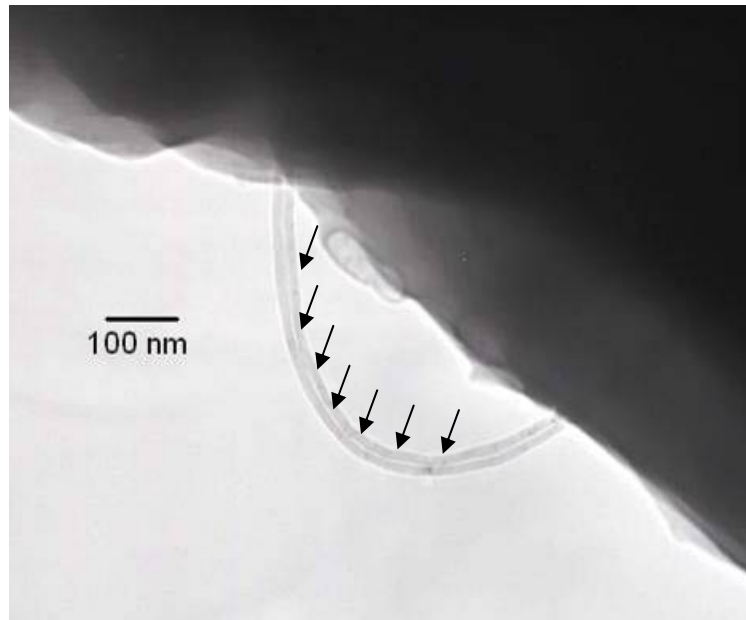


**Figure 12. Buckled nanotube at the fracture surface of the nanocomposite.**

Buckling and collapsing effects of MWCNTs have been previously studied by Wagner *et al.* (1998) [1]. This group characterized an epoxy-based resin that contained MWCNTs under TEM. Wagner's group noticed that the nanotubes buckled and collapsed following the polymerization process of the resin. Furthermore, it was found that mechanical and thermal stresses arising from the polymerization process along with the thermal effects associated with the TEM's electron beam produced this particular phenomenon. Wagner *et al.* (1998) estimated the stresses required to collapse or buckle a nanotube, and found values in the range of 100-150 GPa [1]. The buckling phenomenon observed in the samples supports the idea that there is a strong interface and affinity between the polymeric matrix and the nanotubes. Thus, an effective load transfer from the polymer matrix to the nanotubes exists and therefore, there has been an effective reinforcement of the polymer by introduction of the MWCNTs. More importantly, these hypotheses are supported at the macroscopic level as an improvement in the mechanical properties when compared to unfilled SL resin was observed in the present study.

#### **4. Concluding remarks**

Novel nanocomposite materials consisting of an epoxy-based matrix (DSM Somos commercially available SL resins) and a nanostructured filler material were successfully produced. Complex 3-D geometries were successfully fabricated by means of a modified multi-material SL system. The use of MWCNTs as a reinforcement material for these particular SL resins resulted in a remarkable increase of the ultimate tensile strength, fracture strength, and hardness. These mechanical properties enhancements could result in a new class of high performance SL materials for specific functional applications. Furthermore, these improvements could open new markets and applications for SL and other RP technologies.

One advantage of the non-localized ultrasonic dispersion utilized during this research is that this method does not physically and thus negatively affect the structure of the nanotubes. Electron microscopy showed affinity between the nanocomposite's constituents and strong interfacial bonding effects (buckled nanotubes) were also observed. These effects were reflected at a macroscopic level as an improvement of the mechanical properties when compared to unfilled SL resin. The modified SL machine setup used to manufacture the test specimens and sample parts, allows for testing of a variety of SL resins, nanostructured materials and concentrations without the need for large amounts of materials. The proposed techniques will allow for the future tailoring of the physical properties of SL nanocomposites at large scales.

## Acknowledgments

This research was supported in part by the National Science Foundation, Louis Stokes Alliance for Minority Participation (LSAMP) Bridge to Doctorate Fellowship (JHS and KFS). The research presented here was performed at UTEP in the W.M. Keck Border Biomedical Manufacturing and Engineering Laboratory (W.M. Keck BBMEL) using equipment purchased through Grant Number 11804 from the W.M. Keck Foundation. This material is based in part upon work supported by the Texas Advanced Research (Advanced Technology/Technology Development and Transfer) Program under Grant Number 003661-0020-2003. Support was also provided through the Mr. and Mrs. MacIntosh Murchison Chairs No. I and II (RBW and LEM, respectively). The use of UTEP's Metallurgical and Materials Engineering TEM, SEM and mechanical testing facilities is gratefully acknowledged.

## References

1. Harris, P., "Carbon Nanotubes and Related Structures," Published by Cambridge University Press, UK, 1999.
2. Curran, S.A., Ajayan, P.M., Blau, W.J., Carrol, D.L., Coleman, J.N., Dalton, A.B., Davey, A.P., Drury A, McCarthy B, Maier S, Strevens A; "A Composite from Poly(m-phenylenevinylene-co-2,5-dioctoxy-p-phenylenevinylene) and Carbon Nanotubes: A Novel Material for Molecular Optoelectronics," *Advanced Materials*, 10 (14): 1091-1093, 1998.
3. Andrews, R., Weisenberger, M.C., "Carbon Nanotube Polymer Composites," *Current Opinion in Solid State and Materials Science*, 8, 31-37, 2004.
4. Wicker, R.B., Ranade, A.V., Medina, F., and Palmer, J., "Practical Consideration for Micro-Stereolithography of Embedded Micro-Channels," *Proceedings of the Rapid Prototyping & Manufacturing 2004 Conference*, May 10-13, 2004, Dearborn, Michigan. Also, SME Technical Paper TP04PUB210 (Dearborn, Mich.: Society of Manufacturing Engineers, 2004).
5. Ranade, A.V., "Microstereolithography of Embedded Micro-Channels," University of Texas at El Paso, Department of Mechanical and Industrial Engineering, Master's Thesis, 2005.
6. Lozoya, O.A., "Design and Development of a Retrofitted Multiple Material Stereolithography System," University of Texas at El Paso, Department of Mechanical and Industrial Engineering, Master's Thesis, 2005.

7. Jacobs, P.F., "Stereolithography and other RP & M Technologies from Rapid Prototyping to Rapid Tooling," Published by Society of Manufacturing Engineers in cooperation with the Rapid Prototyping Association of SME, Dearborn, Michigan, 1996.
8. Arcaute, K., Ochoa, L., Medina, F., Elkins, C., Mann, B. and Wicker, R.B., "Three-Dimensional PEG Hydrogel Construct Fabrication using Stereolithography," Materials Research Society Symposium Proceedings, Volume 874, Symposium L, L5.5.1-7, 2005.
9. American Society for Testing and Materials, Standard 638 "Standard Test Method for Tensile Properties of Plastics," Annual Book of ASTM Standards, PA, 1994.
10. Gojny, F.H, Wichmann, M.H.G., Fieldler, B., and Schulte, K., "Carbon Nanotube-Reinforced Epoxy-Composites: Enhanced Stiffness and Fracture Toughness at Low Nanotube Content," Composites Science and Technology 64, 2363–2371, 2004.
11. Davis, J.R., "Tensile Testing," Published by ASM International, Materials Park, Ohio, 2004.
12. Jang, B.Z., "Advanced Polymer Composites: Principles and Applications," Published by ASM International, Materials Park, Ohio, 2004.
13. Gojny, F.H., Nastalczyk, J., Zbigniew, R., and Schulte, K., "Surface Modified Multi-Walled Carbon Nanotubes in CNT/Epoxy-Composites," Chemical Physics Letters, 370, 820-824, 2003.